ESC European Society of Cardiology

Europace (2023) **25**, 496–505
https://doi.org/10.1093/europace/euac222

CLINICAL RESEARCH

Lipomatous metaplasia prolongs repolarization and increases repolarization dispersion within post-infarct ventricular tachycardia circuit cites

Lingyu Xu [1]*, Sohail Zahid[2], Mirmilad Khoshknab[1], Juwann Moss [1], Ronald D. Berger [3,4], Jonathan Chrispin [3,4], David Callans[1], Francis E. Marchlinski [1], Stefan L. Zimmerman [5], Yuchi Han [1], Benoit Desjardins [6], Natalia Trayanova [3], and Saman Nazarian [1]

[1]Cardiovascular Medicine Division, University of Pennsylvania School of Medicine, 3400 Spruce Street, Philadelphia, PA 19104, USA; [2]Department of Internal Medicine, NYU Langone Medical Center, New York, NY, USA; [3]Department of Biomedical Engineering, Johns Hopkins University, Baltimore, MD, USA; [4]Department of Cardiology, Johns Hopkins University, Baltimore, MD, USA; [5]Department of Radiology and Radiological Sciences, Johns Hopkins University, Baltimore, MD, USA; and [6]Department of Radiology, University of Pennsylvania School of Medicine, Philadelphia, PA, USA

Received 3 October 2022; accepted after revision 20 October 2022; online publish-ahead-of-print 15 December 2022

Aims

Post-infarct myocardium contains viable corridors traversing scar or lipomatous metaplasia (LM). Ventricular tachycardia (VT) circuitry has been separately reported to associate with corridors that traverse LM and with repolarization heterogeneity. We examined the association of corridor activation recovery interval (ARI) and ARI dispersion with surrounding tissue type.

Methods and results

The cohort included 33 post-infarct patients from the prospective Intra-Myocardial Fat Deposition and Ventricular Tachycardia in Cardiomyopathy (INFINITY) study. We co-registered scar and corridors from late gadolinium enhanced magnetic resonance, and LM from computed tomography with intracardiac electrogram locations. Activation recovery interval was calculated during sinus or ventricular pacing, as the time interval from the minimum derivative within the QRS to the maximum derivative within the T-wave on unipolar electrograms. Regional ARI dispersion was defined as the standard deviation (SD) of ARI per AHA segment (ARI_{SD}). Lipomatous metaplasia exhibited higher ARI than scar [325 (interquartile range 270–392) vs. 313 (255–374), $P < 0.001$]. Corridors critical to VT re-entry were more likely to traverse through or near LM and displayed prolonged ARI compared with non-critical corridors [355 (319–397) vs. 302 (279–333) ms, $P < 0.001$]. ARI_{SD} was more closely associated with LM than with scar (likelihood ratio χ^2 50 vs. 12, and 4.2-unit vs. 0.9-unit increase in 0.01*Log(ARI_{SD}) per 1 cm^2 increase per AHA segment). Additionally, LM and scar exhibited interaction ($P < 0.001$) in their association with ARI_{SD}.

Conclusion

Lipomatous metaplasia is closely associated with prolonged local action potential duration of corridors and ARI dispersion, which may facilitate the propensity of VT circuit re-entry.

Keywords

Lipomatous metaplasia • Ventricular tachycardia • Activation recovery interval • Myocardial infarction • Ischaemic cardiomyopathy

* Corresponding author. Tel: +1 215 615 5220; Fax: +1 215 615 5235. *E-mail address*: Lingyu.Xu@pennmedicine.upenn.edu

© The Author(s) 2022. Published by Oxford University Press on behalf of the European Society of Cardiology.
This is an Open Access article distributed under the terms of the Creative Commons Attribution-NonCommercial License (https://creativecommons.org/licenses/by-nc/4.0/), which permits non-commercial re-use, distribution, and reproduction in any medium, provided the original work is properly cited. For commercial re-use, please contact journals.permissions@oup.com

What's new?

- Corridors traversing through or near LM exhibit significantly longer repolarization duration than those traversing scar.
- Myocardial LM, but not myocardial scar, is the primary substrate of increased repolarization dispersion during basal rhythm, facilitating VT re-entry.

Introduction

Ventricular tachycardia (VT) is an important cause of mortality in patients with prior myocardial infarction (MI) and ventricular dysfunction. Reduced post-infarct myocardial viability is associated with increased ventricular repolarization dispersion,[1] and the VT substrate has been demonstrated to manifest abnormal ventricular repolarization[2] and increased repolarization heterogeneity.[3,4] The activation recovery interval (ARI), the interval between the local depolarization time and repolarization time, has been demonstrated to be closely associated with action potential duration (APD)[5] and approximates the refractory period.[6] Activation recovery interval derived from intracardiac unipolar electrograms has been widely used as a surrogate of the local APD and refractory period.[2,7]

The prevailing paradigm that scar is the primary substrate for VT re-entry[8] has been challenged by recent findings that myocardial lipomatous metaplasia (LM) is a significant contributor to electrophysiological remodelling in a post-infarct sheep model,[9] as well as human myocardium.[10] Myocardial LM, i.e. metaplasia of adipose tissue from fibrosis within the infarcted myocardium, is widely recognized,[10–12] Similar to scar, it exhibits bright signal on late gadolinium enhancement (LGE) on cardiovascular magnetic resonance (CMR) images[12]; however, it can be readily distinguished on computed tomography (CT).

Previous studies have reported ARI measurements in scar, border zone (BZ) tissue, and remote normal myocardium[2] in small case series of patients with heterogeneous aetiologies of cardiomyopathy. However, comprehensive evaluation of ARI in human post-infarct myocardium and its association with VT conductive corridors surrounded by scar vs. LM has not been performed. In this study, we sought to investigate the association of ARI in conductive corridors and regional ARI dispersion with surrounding infarct tissue type, scar vs. LM, to predict critical VT sites.

Methods

The patient recruitment, CMR and CT image acquisition and analysis protocols, image registration to electroanatomic mapping (EAM) methodology, electrophysiological study, and ablation strategy and statistical analyses for the INFINITY study have been previously reported.[11] The latter methodologies together with the details related to the calculation of ARI from intracardiac unipolar electrograms and regional ARI dispersion, can be found in Supplemental material.

Results

Baseline characteristic

The baseline characteristics are summarized in *Table 1*. Of 23 595 EAM points, 804 on corresponding coordinates on CMR and/or CT images were excluded due to image artefacts (see Supplementary material online, *Table S1*) and 9099 were excluded due to inability to compute ARI because of insufficient waveform. Consequently, the ARI measurements of 13 692 points [median 385, interquartile range (IQR) 217–542 points per patient] were incorporated in the analysis, including 2623 in healthy myocardium (healthy myocardium area from LGE excluding LM distinguished by CT), 4849 in BZ (BZ area from LGE excluding LM), 4868

Table 1 Baseline characteristics ($n = 33$)

Vital statistics	
Age, years	66 ± 8
Male	31 (94%)
Body mass index, kg/m^2	31.2 ± 6.9
Systolic blood pressure, mmHg	116 ± 17
Diastolic blood pressure, mmHg	68 ± 12
Heart rate, beats/min	69 ± 10
Disease history	
Infarction age since the index myocardial infarction, year	17 (4–22)
Heart failure	24 (73%)
New York Heart Association class	2.4 ± 0.7
Hypertension	22 (67%)
Diabetes mellitus	16 (48%)
Other arrhythmia (Afib/AFL or PVC)	19 (58%)
Pulmonary disease	5 (15%)
Renal insufficiency	4 (12%)
Hyperlipidaemia	19 (58%)
Hypothyroidism	9 (27%)
Obstructive sleep apnoea	8 (24%)
Presence of ICD	32 (97%)
Laboratory test	
Serum creatinine, mg/dL	1.2 ± 0.7
Anti-arrhythmic medications	
Amiodarone	23 (70%)
Sotalol	4 (12%)
Digoxin	3 (9%)
Mexiletine	4 (12%)
Quinidine	1 (3%)
Dofetilide	1 (3%)
Other cardiovascular medications	
Anti-platelet	24 (73%)
Anti-coagulation	19 (58%)
Statin	28 (85%)
ACEI or ARB use	32 (97%)
Calcium channel blocker	4 (12%)
Beta-blocker use	28 (85%)
Mineralocorticoid receptor antagonist	13 (39%)
Basic cardiac MRI measurements	
LVEF, %	25 ± 10
LVEDVi, mL/m^2	146 ± 41
LVESVi, mL/m^2	111 ± 41
LV mass index, g/m^2	79 ± 18
RVEF, %	36 ± 12
RVEDVi, mL/m^2	79 ± 16
RVESVi, mL/m^2	51 ± 16

Continuous variables expressed as mean ± SD or median (interquartile range), as appropriate and categorical variables are expressed as number (percentage).
ACEI, angiotensin converting enzyme inhibitor; Afib/AFL, atrial fibrillation/flutter; ARB, angiotensin II receptor blocker; ICD, implantable cardioverter-defibrillators; LVEF, left ventricular ejection fraction; LVEDVi, left ventricular end-diastolic volume index; LVESVi, left ventricular end-systolic volume index; LV mass index, left ventricular mass index; PVC, premature ventricular contraction; RVEF, right ventricular ejection fraction; RVEDVi, right ventricular end-diastolic volume index; RVESVi, right ventricular end-systolic volume index.

Table 2 Tissue-specific impulse activation recovery interval (number of patients = 33)

		Absolute value			Z-score		
		Median (IQR)	Coefficient, β		Median (IQR)	Coefficient, β	
ARI (ms) vs. tissue types, $n = 13\,692$	Normal myocardium $n = 2623$, 18.9%	270 (230–332)	0	Reference	−0.36 (−0.89, 0.33)	0	Reference
	BZ-scar $n = 4849$, 34.9%	294 (244–364)[a]	12	↑	−0.13 (−0.78, 0.50)	0.18	↑
	Dense scar[b] $n = 4868$, 35.0%	313 (255–374)[a,c]	27	↑↑↑	0.06 (−0.60, 0.57)	0.36	↑↑↑
	Minimal LM, $n = 119$, 0.9%, (7.8% of all LM)	280 (246–352)[a,c,d]	21	↑↑	−0.24 (−0.70, 0.56)	0.26	↑↑
	BZ-LM, $n = 499$, 3.6%, (33.3% of all LM)	306 (254–384)[a,c]	34	↑↑↑↑	0.09 (−0.56, 0.79)	0.44	↑↑↑↑
	Dense LM[b], $n = 945$, 6.8%, (58.9% of all LM)	325 (270–392)[a,c,d,e]	41	↑↑↑↑↑	0.13 (−0.51, 0.82)	0.51	↑↑↑↑↑
ARI (ms) vs. scar transmurality, $n = 4658$	Subendocardium only $n = 518$, 11.1%	309 (255, 389)	0	Reference	0.00 (−0.58, 0.75)	0	Reference
	Subendocardium to mid myocardium $n = 1460$, 31.3%	311 (252–382)	5.1	—	0.04 (−0.58, 0.64)	0.057	—
	Subendocardium to subepicardium $n = 2680$, 57.5%	314 (256–373)	8.3	—	0.10 (−0.62, 0.55)	0.081	—
ARI (ms) vs. LM transmurality, $n = 962$	Subendocardium only $n = 251$, 26.1%	310 (245, 389)	0.0	Reference	−0.07 (−0.74, 0.71)	0.0	Reference
	Subendocardium to mid myocardium $n = 252$, 26.2%	310 (250–384)	−5.78	—	−0.02 (−0.68, 0.54)	−0.05	—
	Subendocardium to subepicardium $n = 459$, 47.7%	320 (269–400)[f,g]	17.8	↑	0.21 (−0.50, 1.04)[f,g]	0.19	↑

↑ indicates a significant positive association and the number of arrows indicates the magnitude of association.
ARI, activation recovery interval; BZ, border zone; BZ-LM, LM located within BZ in LGE image; dense LM, LM located within dense LGE in LGE image; LM, lipomatous metaplasia; Minimal LM, LM located within healthy myocardium in LGE image.
[a]Significantly different from normal myocardium.
[b]ARI measurements in dense scar or dense LM, likely reflect the ARI of surviving myocardial strands below the resolution of imaging.
[c]Significantly different from BZ-scar.
[d]Significantly different from dense scar.
[e]Significantly different from BZ-LM.
[f]Significantly different from subendocardium only.
[g]Significantly different from subendocardium to mid myocardium.

in scar (dense LGE area from LGE excluding LM), and 1563 points in LM. The EAM points in LM based on CT were further categorized by corresponding LGE images into: dense LM = 954 (58.9%) located within dense LGE; BZ-LM = 499 (33.3%) located within BZ; minimal LM = 119 (7.8%) located within healthy myocardium. The median surface registration error was 3.2 (1.4–5.6) mm between EAM and LGE and 3.2 (1.5–5.8) mm between EAM and CT images. The correlation between ARI and the co-registered signal intensity of LGE-CMR image (healthy myocardium, BZ, and scar) is non-inferior to the correlation between ARI and bipolar voltage (<0.5 mV for scar, 0.5~1.5 mV for BZ, and >1.5 mV for healthy myocardium),[13] with model χ^2 77 vs. 60, respectively.

Tissue-specific activation recovery interval

The ARI displayed stepwise increase from the normal myocardium, BZ, to scar tissue, with median ARI 270 vs. 294 vs. 313, all pairwise $P < 0.001$. Of all electrograms within LM on CT, the ARI of surviving strands within dense LM was longer than those within scar [325 (270–392) vs. 313 (255–374) ms, $P < 0.001$]; similarly, the ARI within BZ-LM was longer compared with BZ-scar [306 (254–384) vs. 294 (244–364) ms, $P < 0.001$] (*Table 2* and *Figure 1*). These results remained consistent after adjustment with cycle length and rhythm (ventricular pacing vs. sinus rhythm) during mapping (see Supplementary material online, *Table S2*). The ARI derived from unipolar electrograms recorded during ventricular pacing was shorter [median 20 (IQR 16–26) ms] than those recorded during sinus rhythm. However, the percentage of ventricular pacing in each tissue types was similar at 18.8% in normal myocardium vs. 17.8% in minimal LM ($P = 0.36$), 11.6% in BZ-scar vs. 13.3% in BZ-LM ($P = 0.18$), 8.7% in dense scar vs. 8.5% in dense LM ($P = 0.37$). Therefore, there was no imbalance in measurements derived during pacing vs. sinus rhythm by tissue type. The ARI within scar was unassociated with scar transmurality, whereas the ARI within LM prolonged as LM transmurality increased (*Table 2*).

Lipomatous metaplasia proximity with corridors critical for ventricular tachycardia

Of 421 corridors of viable myocardium computed to traverse LGE, 20 corridors were removed from analysis due to ICD lead artefact on the

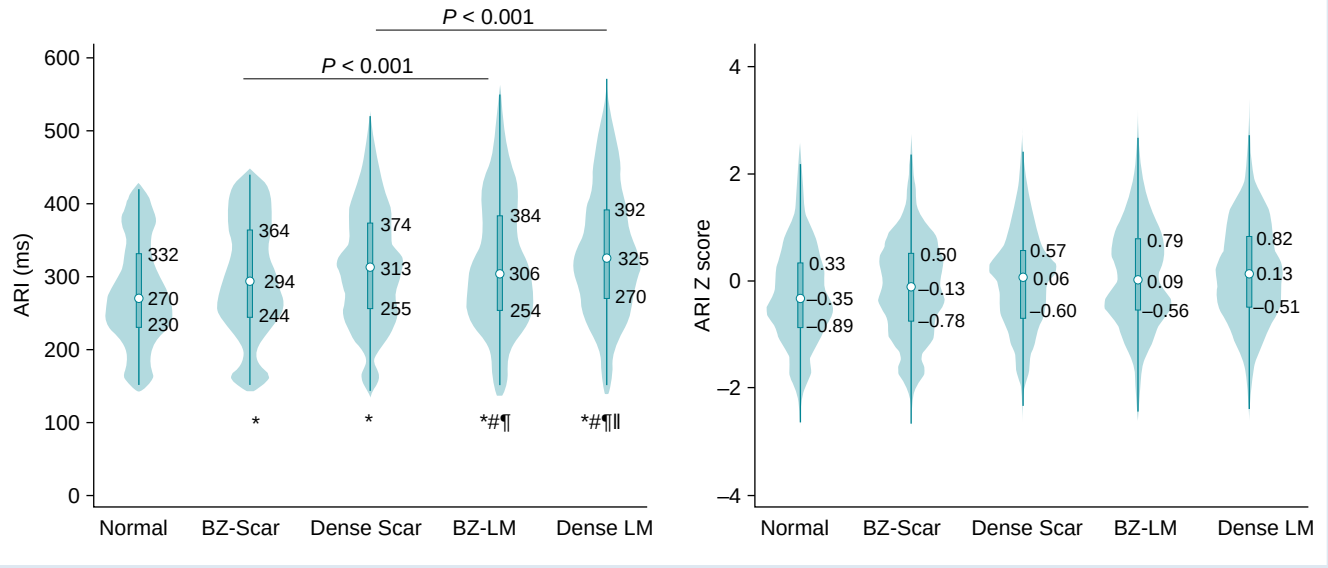

Figure 1 Violin plots of activation recovery interval by tissue types—The figure illustrates violin plots of the absolute value and the Z score (left and right panel, respectively) of activation recovery interval (ARI) by distribution in healthy myocardium, border zone (BZ) tissue, scar and lipomatous metaplasia (LM). The hollow circle shows the median, the box shows the interquartile range, the whiskers extend to the upper and lower adjacent values, and the shaded regions indicate the entire data density distribution. ARI measurements in dense scar or LM likely reflect the ARI of surviving strands within LM or scar beyond the limits of MRI resolution. * means significantly different from normal myocardium; # means significantly different from border zone tissue; ¶ means significantly different from dense scar; ‖ means significantly different from BZ-LM; BZ-LM: LM located within BZ in LGE image. Dense LM: LM located within dense LGE in LGE image. LM, lipomatous metaplasia; BZ, border zone; ARI, activation recovery interval.

septum on cardiac CT, which prohibited LM analysis (see Supplementary material online, *Table S1*). Similar to previously reported data from a smaller subset of the cohort,[11] 98 out of 102 (96%) critical VT corridors traversed through or were adjacent to LM (*Figure 2, C1*), while 272 out of 299 (91%) non-critical corridors were distant from LM (*Figure 2, C2*).[11] Among corridors critical for VT, which traversed LM, 95 had ARI measurements at successive points along the corridor (*Figure 2, A1–C1*) with longer ARI_{mean} [355 (319–397) vs. 302 (277–333) ms, $P < 0.001$] and higher ARI_{SD} [61 (35–78) ms vs. 38 (21–60) ms, $P < 0.001$], when compared with 117 non-critical corridors distant from LM (*Table 3*, *Figure 2F*). We observed that a corridor $ARI_{mean} \geq 362$ ms discriminates corridors critical for VT re-entry, with sensitivity of 0.86 and specificity of 0.89. Additionally, a corridor $ARI_{SD} \geq 53$ ms discriminates corridors critical for VT re-entry with a sensitivity of 0.85 and specificity of 0.86 (see Supplementary material online, *Figure S1*).

Lipomatous metaplasia vs. scar association with activation recovery interval dispersion

Among a total of 5049 AHA segments, 4408 segments had registered EAM points. After excluding 171 segments due to image artefact (see Supplementary material online, *Table S1*) and 175 AHA segments due to incomputable ARI measurements, a total number of 4062 AHA segments were incorporated into the multilevel model analysis, with a median 17 (8–40) EAM points per AHA segment. The number of critical VT sites per AHA segment was associated with regional ARI dispersion (*Figure 3A*) and exhibited strong association with regional LM area per segment but substantially less with regional scar area (*Figure 3B*). Importantly, the regional LM area had a stronger magnitude of association with regional ARI dispersion, when compared with scar (*Figure 3C*), with the △AIC of two models >10 (*Figure 3D*), but LM had strong interaction with scar ($P < 0.001$). Lipomatous metaplasia and scar also exhibited added value over each other in predicting ARI dispersion (*Figure 3E*). A 4.2- and 0.9-unit increase of $Log(ARI_{SD})/100$ was detected in every 1 cm^2 increase of regional LM and scar area, respectively. Mediation analyses revealed that 3% of regional LM area effect on regional critical VT sites was mediated by ARI dispersion (*Figure 3F*), and 19% of regional ARI effect on regional critical VT sites was mediated by regional LM area (*Figure 3G*).

Regional activation recovery interval duration vs. activation recovery interval dispersion association with critical ventricular tachycardia sites

Regional ARI duration, the mean ARI per AHA segment, was positively associated with the regional critical VT sites (*Figure 4B*). Mediation analyses revealed that 31% of the regional ARI duration effect on regional critical VT sites was mediated by regional ARI dispersion (*Figure 4C*). However, only 9% of the regional ARI dispersion effect on regional critical VT sites was mediated by regional ARI duration (*Figure 4D*). Regional ARI dispersion exhibited significantly stronger association with regional critical VT sites compared to regional ARI duration, with the △AIC of two models 116 > 10 (*Figure 4E*). Regional ARI duration was no longer a predictor of regional critical VT sites when adjusted with regional ARI dispersion and exhibited no added value over regional ARI dispersion (*Figure 4F*).

Discussion

This is the first study to investigate the association of myocardial ARI with surrounding LM vs. scar and its impact on VT re-entry. Our

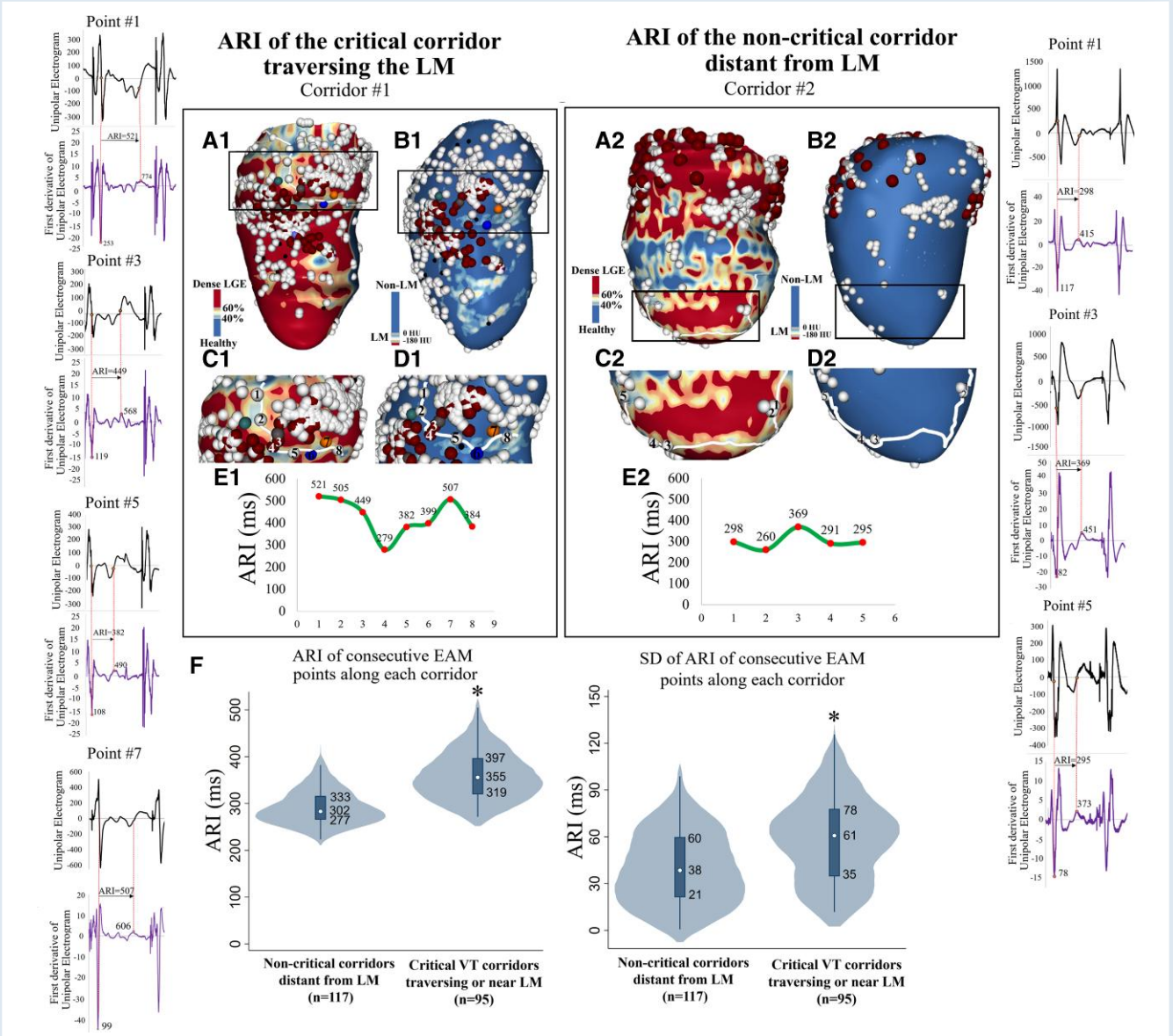

Figure 2 Examples of ARI along corridors participating in VT re-entry circuits versus corridors not participating in VT circuits. (*A*, 1 and 2) Corridors (white line) computed from LGE image, with the corridor magnified (square box) in (*C*). (*B*, 1 and 2) Visualization of lipomatous metaplasia (LM, white area) in CT image, with the corresponding part of the corridor from the (A) magnified in (*D*). (*D*, 1 and 2) The corridor (white line) in relation to LM. (*E*, 1 and 2) Activation recovery interval (ARI) measurements of intracardiac electrogram points along the corridors are displayed in a scatter plot, showing substantially longer ARI and higher ARI_{SD} along Corridor 1 (critical to VT circuitry) compared to Corridor 2 (not critical to VT circuitry). (*F*) Violin plot of the ARI_{Mean} and ARI_{SD} of measurements at multiple points along corridors traversing or adjacent to the LM found to participate in VT re-entry on entrainment or pace-mapping are significantly higher (indicated as *) than those of corridors distant from LM and not participating in VT re-entry. White points: mapping spots; red points: ablation sites; black points: delayed potential; Point #6 & 7 in Corridor #1: isthmus sites of VT re-entry. The unipolar electrograms and corresponding first derivative graph of every second consecutive points along the corridor are plotted. LM, lipomatous metaplasia; ARI, activation recovery interval; SD, standard deviation.

findings are summarized as follows: (i) post-infarct corridors that support VT re-entry traverse through or near LM and exhibit substantially prolonged repolarization and increased repolarization heterogeneity when compared with non-critical corridors; (ii) LM is more closely associated with regional ARI dispersion than scar, but interacts with scar in its association with ARI dispersion.

Activation recovery interval of regions with lipomatous metaplasia

In this study, we confirmed that ARI was prolonged at each transition from normal myocardium, to BZ, to scar, consistent with data from previous studies.[2] We also showed that ARI within LM is prolonged

Table 3 Late gadolinium enhancement -derived corridors and activation recovery interval along the corridors

Corridors ($n = 401$)	Traverse or adjacent to LM	Number of corridors with measurable ARI	Number of the EAM points along each corridor	Average ARI along each corridor (ms)	ARI SD along each corridor (ms)
VT critical corridors ($n = 102$)	LM (+), $n = 98$, 96%	95	7 (6–9)	355 (319–397)[a]	61 (35–78)[a]
	LM (−), $n = 4$, 4%	4	8 (5–8)	349 (301–386)	36 (20–42)
Non-critical corridors ($n = 299$)	LM (+), $n = 27$, 9%	23	4 (3–6)	335 (303–371)	39 (14–65)
	LM (−), $n = 272$, 91%	117	5 (4–6)	302 (277–333)	38 (21–60)

ARI, activation recovery interval; LM, lipomatous metaplasia; SD, standard deviation; VT, ventricular tachycardia.
[a]Significantly different from non-critical circuits distant from LM, with $P < 0.05$ after Bonferroni correction.

further, compared with that in scar. Homogenous scar and adipose tissue are non-conductive; however, post-infarct scar and LM results in a complex network of scar, BZ, LM, and surviving tissue. The scar and LM interlace with surviving myocardial strands forming complicated conductive paths that propagate electrical impulses,[14] and we believe that the ARI measured within 'dense' LM or scar represents the ARI of the surviving myocardial strands interspersed within LM and scar, which are below current limits of MRI imaging resolution. Surviving myocardial strands within dense LM exhibit longer ARI than those within dense scar, possibly because of increased Connexin 43 lateralization and attenuated myocardial continuity of the surviving myocardial strands within LM.[9] Similarly, regions of BZ-LM displayed prolonged ARI compared with that of BZ tissue.

Lipomatous metaplasia mediates activation recovery interval prolongation within ventricular tachycardia re-entry corridors

We have previously shown that most corridors critical for VT re-entry traverse through or near LM.[11] Corridors extracted from LGE that traversed through or near LM on CT, exhibited prolonged ARI and higher ARI dispersion compared with corridors distant from LM, consistent with the observation that ARI in BZ-LM tissue is prolonged compared with BZ-scar tissue.

Re-entrant VT initiation and maintenance require a balanced interaction between activation and repolarization. Ventricular repolarization is a critical stage of the electrical activity during the cardiac cycle, which functions as a recovery period for the ions to return to the resting state and resets excitability for the next cardiac cycle.[4] The corridors traversing through or near LM exhibit prolonged ARI, and can create unidirectional block. Therefore, a premature impulse traversing towards a corridor surrounded by LM can be unidirectionally blocked when encountering prolonged refractoriness at its proximal side, and may detour around the block and approach the corridor from its distal side.[15] If the impulse conduction is slow enough and is granted proper timing to enter the distal side, which has recovered from refractoriness, re-entrant arrhythmia can be initiated and perpetuated. Additionally, in the current study, LM surrounding the corridors also exhibit increased dispersion of refractory periods, which also enhances the likelihood for VT perpetuation.[16] Our findings indicate that LM electrophysiologically remodels the surviving tissue within, by prolonging ARI duration and increasing ARI dispersion, thus promoting re-entry.

A recent study by Callans and Donahue[17] elucidated that the ARI of post-infarct VT isthmus was shorter than the ARI of scar. Notably, the former study focused on the ARI of isthmus vs. bystander scar sites, whereas our study compared the ARI of critical vs. non-critical corridors within infarct zone. Our tissue-specific findings are consistent with Callans and Donahue's conclusion that the ARIs of VT isthmus (within scar or BZ but close to LM[11]) are shorter than the ARI of EAM points within low voltage zones (dense scar or LM). The current study expands on prior reports by showing that the ARI of critical VT corridors traversing through or near LM is longer than that of non-critical VT corridors distant from LM.

Lipomatous metaplasia and activation recovery interval dispersion in re-entrant tachycardia

In this study, we confirm that regional ARI dispersion is associated with VT re-entry, a finding that is consistent with the vast majority of prior studies.[3,16] We also show that critical VT sites are more closely associated with regional LM area than with scar area, which is consistent with our prior report that critical VT corridors predominantly traverse through or near LM.[11] The present study is also the first, to our knowledge, to report that LM exhibited a stronger association with regional ARI dispersion than scar but exhibits significant multiplicative interaction with scar tissue in this association. These findings indicate that while scar plays a secondary role to LM, its presence enhances the anatomic substrate for creating local ARI dispersion to facilitate re-entrant arrhythmia. However, only 3% of the regional LM area effect on critical VT sites was mediated by ARI dispersion, indicating important other means by which LM contributes to the electrical substrate for re-entry, by reducing current loss[11] and slowing the conduction velocity[9] in the VT re-entry pathway. In contrast, 19% of the ARI dispersion effect on critical VT sites was mediated by regional LM area, indicating that LM appears to be a critical anatomic substrate for increased ARI dispersion. We also found that LM transmurality, but not scar transmurality, is closely associated with increased transmural ARI variability, a finding that mechanistically explains the association of LM with ARI dispersion.

Regional activation recovery interval length and activation recovery interval dispersion in re-entrant tachycardia

In the present study, the ARI of critical corridors was prolonged when compared with the non-critical corridors, and an increased regional ARI

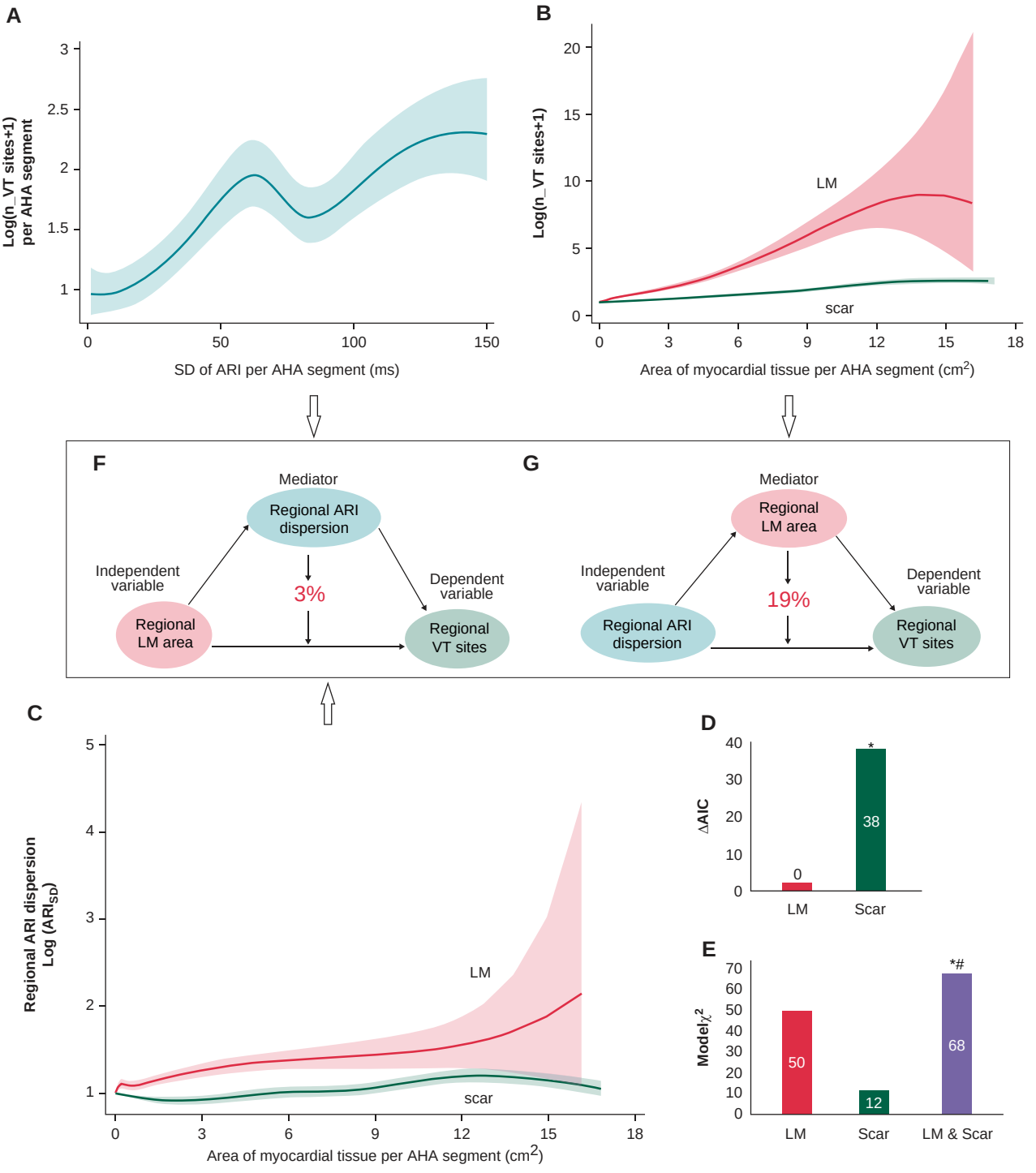

Figure 3 Association between lipomatous metaplasia (LM) area, region activation recovery interval (ARI) dispersion, and number of critical ventricular tachycardia (VT) sites per AHA segment (*A*). Restricted cubic spline (RCS) model with 95% confidence interval boundary shows that regional ARI dispersion (ARI_{SD} per AHA segment) is positively associated with regional critical VT sites [Log (number of VT sites + 1) per AHA segment]. (*B*) The RCS model shows that regional LM area exhibits more positive association with regional critical VT sites than regional scar area. (*C*) The RCS model shows that regional LM area exhibits a more positive association with ARI dispersion than scar area. (*D*) LM exhibits a lower AIC value, with $\triangle$AIC = 38 > 10 when compared with scar area, to predict regional ARI dispersion. (*E*) LM and scar have incremental value over each other when predicting regional ARI dispersion. (*F*) Regional ARI dispersion partially (3%) but significantly mediates the effect of regional LM area on regional critical VT sites. (*G*) Regional LM area partially (19%) but significantly mediates the effect of ARI dispersion on regional critical VT sites. *Significantly different from scar. #Significantly different from LM. AIC, Akaike information criterion; ARI, activation recovery interval; BZ, border zone; LM, lipomatous metaplasia; SD, standard deviation.

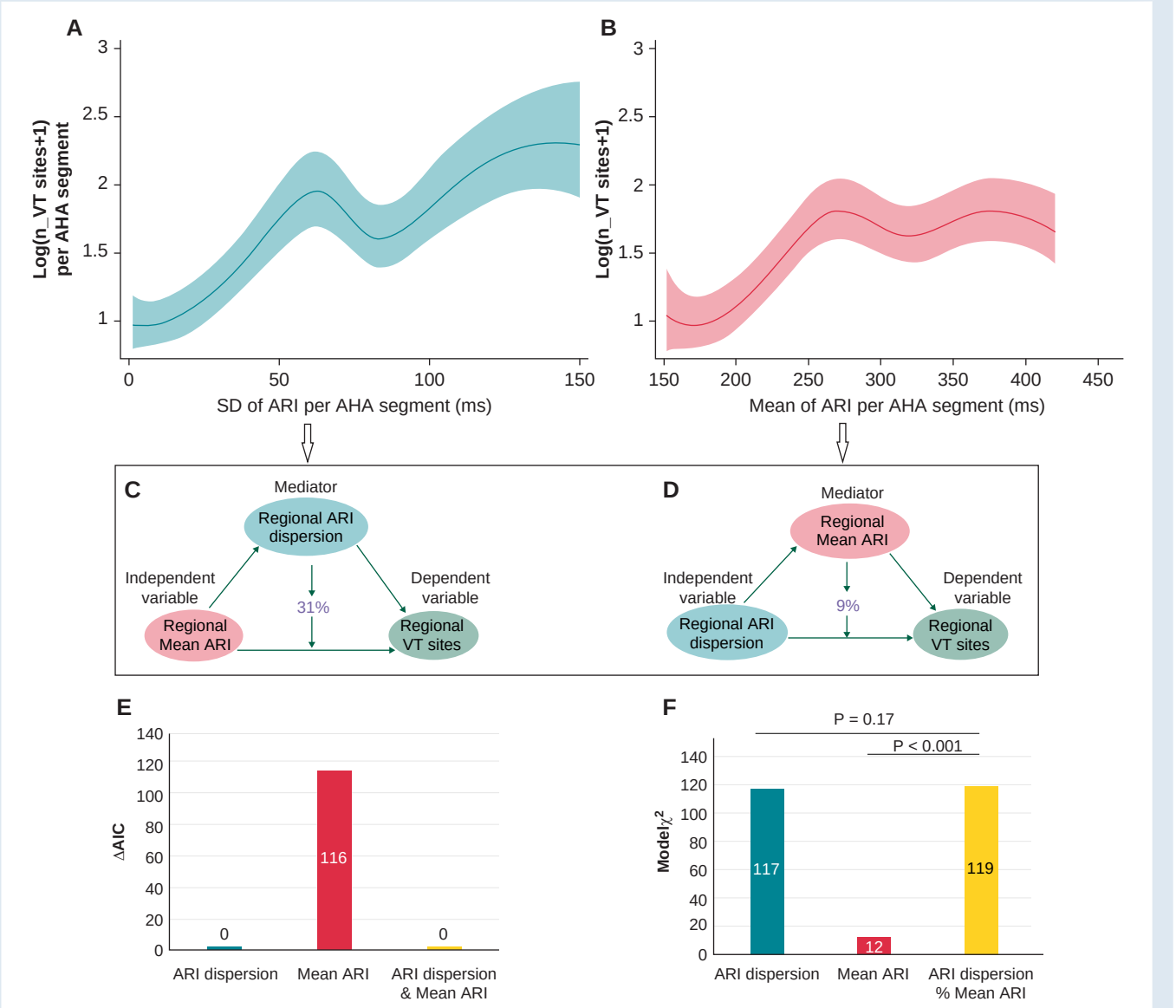

Figure 4 Association between regional activation recovery interval (ARI) dispersion, mean of ARI duration, and number of critical ventricular tachycardia (VT) sites per AHA segment. (*A*) Restricted cubic spline (RCS) model with 95% confidence interval boundary shows that regional ARI dispersion (ARI_{SD} per AHA segment) is positively associated with regional critical VT sites [Log (number of VT sites + 1) per AHA segment]. (*B*) The RCS model shows that the mean of ARI duration per AHA segment exhibits positive, but with a substantially less degree of association with regional critical VT sites than regional ARI dispersion. (*C*) Regional ARI dispersion partially (31%) but significantly mediates the effect of regional mean ARI duration on regional critical VT sites. (*D*) Regional mean ARI only partially (9%) mediates the effect of ARI dispersion on regional critical VT sites. (*E*) Regional ARI dispersion exhibits a lower AIC value with △AIC 116 > 10 when compared with the regional mean of ARI duration to predict regional critical VT sites. (*F*) Regional ARI dispersion has incremental value over the regional mean ARI duration when predicting regional critical VT sites. However, the regional mean of ARI has no incremental value over regional ARI dispersion. AIC, Akaike information criterion; ARI, activation recovery interval; LM, lipomatous metaplasia; SD, standard deviation.

dispersion was also associated with regional VT critical sites. Consequently, we explored the difference in the association between regional ARI duration vs. regional ARI dispersion with critical VT sites. We found that regional ARI dispersion exhibited a substantially more robust association with critical VT sites compared with regional ARI duration. This finding likely explains the fact that anti-arrhythmic drugs with disparate effects on the ARI duration have similar effects on VT suppression because by shortening or prolonging the ARI duration homogeneously, they decrease ARI dispersion, thus making the substrate less susceptible to re-entry.[18,19] Although a prolonged regional ARI is pro-arrhythmic, increased regional ARI dispersion is far more pro-arrhythmic than the prolonged regional ARI duration.

Clinical implications

As corridors participating in VT predominantly traverse through or LM, which potentially helps VT substrate targeting during the ablation, the presence of the corridors traversing or near LM might indicate the

necessity of prophylactic ICD implantation in post-MI patients. As LM, but not scar, is a primary anatomic substrate of regional refractory period dispersion and prolonged ARI of the critical VT corridor, cardiac adipogenesis may be a novel therapeutic target. As regional refractory period dispersion is more pro-arrhythmic than a prolonged refractory period, narrowing the regional refractoriness variability might more effectively eliminate VT re-entry rather than shortening ARI duration.

Limitations

The present study has several limitations. The results should be externally validated in a larger patient cohort. This prospective study aims to evaluate the association of ARI property of critical VT corridors with proximity to LM and unveil the corresponding mechanism, rather than investigating the clinical utility of targeting corridors traversing LM or the ARI mapping. Consequently, LM location and ARI data were not provided to operators. The clinical utility of targeting LM-corridor mapping and ARI mapping should be further validated, and the post-ablation VT re-occurrence and sudden cardiac death should be follow up in the future study. Image artefacts due to motion or defibrillator components may have impacts upon scar and/or LM identification, but there is no reason to suspect that scar vs. LM would have been differentially impacted by such artefacts. The median registration error was 3.2 mm; however, the ARI exhibited a non-inferior level of correlation compared with the correlation between bipolar amplitude and LGE signal intensity, which indicated that the registration error should not influence our findings. Intracardiac points were acquired using point-by-point mapping. Future studies using multipolar catheters may enhance the resolution of electrogram data. Activation recovery interval was not computable in ~40% unipolar electrograms, but levels of missing ARI were similar (37–41%) in each type of myocardial tissue and, therefore, should not cause differential bias. Autonomic tone,[20] heart rate, rhythm, and pacing output might affect ventricular refractoriness; however, similar levels of sedation were utilized in all cases and complete autonomic block is not feasible during VT ablation procedures. Current strength was standardized for each patient when pacing during endocardial mapping. Additionally, the difference of the ARI in LM vs. scar remained unchanged after adjustment for cycle length or rhythm (paced or sinus). We did not explore the impact of ventricular pacing and sinus rhythm (exhibiting a median difference of 20 ms of ARI) in ARI of the corridors and ARI dispersion. However, the ratio of points acquired during pacing vs. sinus rhythm was non-differential with regard to tissue type. Furthermore, the standard deviation of the ARI in sinus rhythm vs. ventricular pacing were both ~90 ms. Consequently, we believe that the basal rhythm has trivial if any impact on the comparison of corridor ARI and ARI dispersion. Activation recovery interval was not measured continuously along the corridor; however, ARI was measured at a median of seven consecutive points along critical and five consecutive points along non-critical corridors, which we believe was sufficient to represent the corridors. Eight out of 98 critical VT circuits identified by intracardiac mapping did not correspond to a corridor on the LGE image. This is likely mediated by the inability of our image resolution to detect markedly thin myocardial corridors. Finally, 70% of patients were on amiodarone prior to the procedure. Due to its long elimination half-life, and lipophilic properties, residual amiodarone may exist in tissues and LM even after 2-week pre-procedural discontinuation. However, our conclusions would likely remain unchanged if amiodarone effect is completely eliminated, because local ARI dispersion would be even larger.

Conclusion

Corridors traversing through or near LM exhibit significantly longer repolarization duration, and LM primarily contributes to higher repolarization dispersion during basal rhythm, facilitating VT re-entry.

Supplementary material

Supplementary material is available at *Europace* online.

Acknowledgements

The authors acknowledge the support from the Mark Marchlinski Electrophysiology Research and Education Fund.

Funding

This work was supported by National Institute of Health [1R01HL142893-01].

Conflict of interest: S.N. is a consultant for CardioSolv and Circle CVI; and principal investigator for research funding from Biosense Webster, ImriCor, Siemens, ADAS software, and the US NIH. F.E.M. has served as consultant for Abbott Medical, Biosense Webster, Biotronik, and Medtronic Inc. The University of Pennsylvania Conflict of Interest Committee manages all commercial arrangements. The remaining authors have declared no conflicts of interest.

Data availability

The data supporting this article will be shared on reasonable request to the corresponding author.

References

1. Ikonomidis I, Athanassopoulos G, Karatasakis G, Manolis AS, Marinou M, Economou A *et al.* Dispersion of ventricular repolarization is determined by the presence of myocardial viability in patients with old myocardial infarction—a dobutamine stress echocardiography study. *Eur Heart J* 2000;**21**:446–56.
2. Srinivasan NT, Orini M, Providencia R, Dhinoja MB, Lowe MD, Ahsan SY *et al.* Prolonged action potential duration and dynamic transmural action potential duration heterogeneity underlie vulnerability to ventricular tachycardia in patients undergoing ventricular tachycardia ablation. *Europace* 2019;**21**:616–25.
3. Porter B, Bishop MJ, Claridge S, Child N, Van Duijvenboden S, Bostock J *et al.* Left ventricular activation-recovery interval variability predicts spontaneous ventricular tachyarrhythmia in patients with heart failure. *Heart Rhythm* 2019;**16**:702–9.
4. Monitillo F, Leone M, Rizzo C, Passantino A, Iacoviello M. Ventricular repolarization measures for arrhythmic risk stratification. *World J Cardiol* 2016;**8**:57–73.
5. Yue AM, Paisey JR, Robinson S, Betts TR, Roberts PR, Morgan JM *et al.* Determination of human ventricular repolarization by noncontact mapping: validation with monophasic action potential recordings. *Circulation* 2004;**110**:1343–50.
6. Millar CK, Kralios FA, Lux RL. Correlation between refractory periods and activation-recovery intervals from electrograms—effects of rate and adrenergic interventions. *Circulation* 1985;**72**:1372–9.
7. Coronel R, de Bakker JM, Wilms-Schopman FJ, Opthof T, Linnenbank AC, Belterman CN *et al.* Monophasic action potentials and activation recovery intervals as measures of ventricular action potential duration: experimental evidence to resolve some controversies. *Heart Rhythm* 2006;**3**:1043–50.
8. Debakker JMT, Vancapelle FJL, Janse MJ, Wilde AAM, Coronel R, Becker AE *et al.* Reentry as a cause of ventricular-tachycardia in patients with chronic ischemic heart-disease—electrophysiologic and anatomic correlation. *Circulation* 1988;**77**:589–606.
9. Pouliopoulos J, Chik WW, Kanthan A, Sivagangabalan G, Barry MA, Fahmy PN *et al.* Intramyocardial adiposity after myocardial infarction: new implications of a substrate for ventricular tachycardia. *Circulation* 2013;**128**:2296–308.
10. Sasaki T, Calkins H, Miller CF, Zviman MM, Zipunnikov V, Arai T *et al.* New insight into scar-related ventricular tachycardia circuits in ischemic cardiomyopathy: fat deposition after myocardial infarction on computed tomography-a pilot study. *Heart Rhythm* 2015;**12**:1508–18.
11. Xu L, Khoshknab M, Berger RD, Chrispin J, Dixit S, Santangeli P *et al.* Lipomatous metaplasia enables ventricular tachycardia by reducing current loss within the protected corridor. *JACC Clin Electrophysiol* 2022;**8**:1274–1285.
12. Kellman P, Hernando D, Arai AE. Myocardial fat imaging. *Curr Cardiovasc Imaging Rep* 2010;**3**:83–91.
13. Santangeli P, Marchlinski FE. Substrate mapping for unstable ventricular tachycardia. *Heart Rhythm* 2016;**13**:569–83.
14. Rog-Zielinska EA, Norris RA, Kohl P, Markwald R. The living scar—cardiac fibroblasts and the injured heart. *Trends Mol Med* 2016;**22**:99–114.
15. Child N, Bishop MJ, Hanson B, Coronel R, Opthof T, Boukens BJ *et al.* An activation-repolarization time metric to predict localized regions of high susceptibility to reentry. *Heart Rhythm* 2015;**12**:1644–53.

16. Callans DJ. *Josephson's clinical cardiac electrophysiology: techniques and interpretation*. 6th ed. Philadelphia, PA: LWW; 2020.
17. Callans DJ, Donahue JK. Repolarization heterogeneity in human post-infarct ventricular tachycardia. *JACC Clin Electrophysiol* 2022;**8**:713–8.
18. Singh BN. Amiodarone and homogeneity of ventricular repolarization and refractoriness. *J Cardiovasc Pharmacol Ther* 1996;**1**:265–70.
19. Vassallo P, Trohman RG. Prescribing amiodarone: an evidence-based review of clinical indications. *JAMA* 2007;**298**:1312–22.
20. Prystowsky EN, Jackman WM, Rinkenberger RL, Heger JJ, Zipes DP. Effect of autonomic blockade on ventricular refractoriness and atrioventricular nodal conduction in humans. Evidence supporting a direct cholinergic action on ventricular muscle refractoriness. *Circ Res* 1981;**49**:511–8.

Erratum

https://doi.org/10.1093/europace/euac251
Online publish-ahead-of-print 15 December 2022

Erratum to: Worldwide trends in antithrombotic therapy prescribing for atrial fibrillation: observations on the 'transition era' to non-vitamin K antagonist oral anticoagulants

This is an Erratum to: Leona A Ritchie, Deirdre A Lane, Gregory Y H Lip, Worldwide trends in antithrombotic therapy prescribing for atrial fibrillation: observations on the 'transition era' to non-vitamin K antagonist oral anticoagulants, *EP Europace*, Volume 24, Issue 6, June 2022, Pages 871–873, https://doi.org/10.1093/europace/euab313

In the originally published version of this manuscript, the following sentence was incorrect:

Non-vitamin K antagonists continue to be the only treatment option in people with antiphospholipid syndrome, advanced chronic kidney disease (creatinine clearance <15 mL/min), rheumatic mitral valve disease, or mechanical heart valves.

The sentence has been corrected online as follows:

Vitamin K antagonists continue to be the only treatment option in people with antiphospholipid syndrome, advanced chronic kidney disease (creatinine clearance <15 mL/min), rheumatic mitral valve disease, or mechanical heart valves.

© The Author(s) 2022. Published by Oxford University Press on behalf of the European Society of Cardiology. All rights reserved. For permissions, please email: journals.permissions@oup.com.